Hindawi Publishing Corporation
International Journal of Photoenergy
Volume 2012, Article ID 139739, 9 pages
doi:10.1155/2012/139739

Research Article

Preparation, Characterization, and Activity Evaluation of CuO/F-TiO_2 Photocatalyst

Zhang Jinfeng,[1] Yang Yunguang,[2] and Liu Wei[2]

[1] *Department of Physics, Huaibei Normal University, Anhui, Huaibei 235000, China*
[2] *Department of Chemistry, Huaibei Normal University, Anhui, Huaibei 235000, China*

Correspondence should be addressed to Liu Wei, weiliu@chnu.edu.cn

Received 21 November 2011; Accepted 31 December 2011

Academic Editor: Baibiao Huang

CuO/F-TiO_2 nanoparticle photocatalyst was prepared by ball milling. The photocatalyst was characterized by X-ray powder diffraction, scanning electron microscopy, transmission electron microscopy, UV-Vis diffuse reflectance spectroscopy, and photoluminescence emission spectroscopy. The photocatalytic activity was evaluated by photocatalytic oxidation of rhodamine B and reduction of $Cr_2O_7^{2-}$. The results showed that, for F-TiO_2 photocatalyst, the photooxidation activity increases remarkably with the increasing amount of NH_4F up to 1.0 g, and the photoreduction activity decreases gradually with the increase in the amounts of NH_4F. For the CuO/F-TiO_2 photocatalyst, the photoreduction activity increases greatly with the increase in the amount of doped p-CuO up to 1.0 wt.%, and the photooxidation activity decreases rapidly with the increase in the amounts of doped p-CuO. Compared with pure TiO_2, the photoabsorption wavelength range of the CuO/F-TiO_2 and F-TiO_2 photocatalysts red shifts and improves the utilization of the total spectrum. The effect of ball milling time on the photocatalytic activity of the photocatalysts was also investigated. The mechanisms of influence on the photocatalytic activity of the photocatalysts were also discussed.

1. Introduction

Since Fujishima and Honda discovered the photocatalytic splitting of water on titanium dioxide (TiO_2) electrodes in 1972 [1], TiO_2 as a photocatalyst has been extensively studied because it has relatively high photocatalytic activity, biological and chemical stability, low cost, nontoxicity, and long-term stability against photocorrosion and chemical corrosion [2–9]. However, the photocatalytic activity of TiO_2 is limited to irradiation wavelengths in the UV region, thus the effective utilization of solar energy is limited to about 3–5% of the total solar spectrum. Some problems still remain to be solved in its application, such as the fast recombination of photogenerated electron-hole pairs. Therefore, improving photocatalytic activity by modification has become a hot topic among the researchers in the near decade [10, 11]. Many investigators have quested for various methods, such as doping transition metals [12–15], doping nonmetallic elements [16–20], and forming composite photocatalysts from different semiconductors [21–24], and so forth, to enhance the photocatalytic activity of TiO_2 and to improve the utilization of visible light.

Recently, fluorinated TiO_2 (F-TiO_2) had been investigated extensively. The results showed that the photocatalytic oxidation activity of the F-TiO_2 is much higher than that of TiO_2 by reason of the extension of the photoabsorption wavelength as a result of doped F element [25–27]. The p-n junction photocatalysts NiO/TiO_2 and p-ZnO/n-TiO_2 have been studied in our laboratory [21, 28]. The results showed that, compared with pure TiO_2, the p-n junction photocatalysts have higher photocatalytic reduction activity, but lower photocatalytic oxidation activity. It is known that CuO is a p-type semiconductor [29]. When p-type CuO and fluorinated n-type TiO_2 integrates, a p-n heterojunction photocatalyst CuO/F-TiO_2 will be formed, which may improve charge separation and photocatalytic activity of the photocatalyst.

In this paper, CuO/F-TiO_2 powder was prepared by ball milling using NH_4F solution as a disperser. The photocatalytic activity of the photocatalyst was evaluated by photocatalytic oxidation of rhodamine B (RhB) and reduction of $Cr_2O_7^{2-}$. The desired result was obtained. The effect of ball milling time on the photocatalytic activity of the photocatalysts was also investigated. The mechanisms of

influence on the photocatalytic activity of the CuO/F-TiO_2 photocatalyst were also discussed.

2. Experimental

2.1. Materials. The TiO_2 powder (Anatase 90%, Rutile 10%, with crystallite size of about 50–60 nm) used in the experiments was supplied by Sinopharm Chemical Reagent Co, Ltd. $Cu(NO_3)_2 \cdot 3H_2O$ was supplied by Shanghai Reagent Factory (purity 99.9%). NH_4F, Rhodamine B, and other chemicals used in the experiments were purchased from Shanghai and other China Chemical Reagent Ltd. They were of analytically pure grade. Deionized water was used throughout this study.

2.2. Preparation of F-TiO_2 and CuO/F-TiO_2. Nanoparticle CuO was synthesized by heat treatment of $Cu(NO_3)_2 \cdot 3H_2O$ at 500°C for 6 h in air, and the crystallite size is about 80 nm. The preparation of F-TiO_2 photocatalyst was carried out in a ND2-2L ball mill (made in Tianzun Electronics Co, Ltd., Nanjing University). The procedures for the preparation of F-TiO_2 are as follows: 5.0 g TiO_2 powder and three different sizes of zirconia balls were mixed in the zirconia tank, and then a certain amount of NH_4F (0 g, 0.2 g, 0.5 g, 1.0 g, 1.5 g, 2.0 g, 2.5 g) and H_2O (5 mL) was added. After being milled for a certain time (0–24 h) at the speed of 550 rpm, the wet powder was dried at 110°C in air. The final samples were used for the determination of photocatalytic activity and characterization. CuO/F-TiO_2 photocatalyst was prepared in the same procedure. For each sample, 1.0 g NH_4F, 5.0 g TiO_2, and 5.0 mL H_2O were added in a zirconia tank, varying the weight ratio of CuO(0 wt.%, 0.1 wt.%, 0.3 wt.%, 0.5 wt.%, 1.0 wt.%, 3.0 wt.%, and 5.0 wt.%), and then different CuO/F-TiO_2 powder samples were prepared, respectively. The specific surface area of the different CuO/F-TiO_2 photocatalysts has no obvious change and it is about 24.7 m^2/g. The flow chart of preparation of the CuO/F-TiO_2 is given in Scheme 1.

2.3. Photoreaction Apparatus and Procedure. Experiments were carried out in a photoreaction apparatus [21, 28]. The photoreaction apparatus consists of two parts. The first part is an annular quartz tube. A 375 W medium pressure mercury lamp (Institute of Electric Light Source, Beijing), with a maximum emission at about 365 nm, was used as light sources. The lamp is laid in the empty chamber of the annular tube, and running water passes through an inner thimble of the annular tube. Owing to continuous cooling, the temperature of the reaction solution is maintained at approximately 30°C. The second part is an unsealed beaker with a diameter of 12 cm. At the start of the experiment, the reaction solution (volume, 300 mL) containing reactants and photocatalyst was put in the unsealed beakers, and a magnetic stirring device was used to stir the reaction solution. The distance between the light source and the surface of the reaction solution is 11 cm. In the experiments, the initial pH of the reaction solution was 5.0, the amount of the photocatalyst used was 2.0 g/L, and the initial concentrations of $Cr_2O_7^{2-}$ and RhB were 1.0×10^{-4} and 1.0×10^{-5} mol/L, respectively. In order to disperse the photocatalyst powder, the suspensions were ultrasonically vibrated for 10 or 20 min prior to irradiation. After illumination, the samples taken from the reaction suspension were centrifuged at 7000 rpm for 20 min and filtered through a 0.2 μm millipore filter to remove the particles. The filtrate was then analyzed. In order to determine the reproducibility of the results, at least duplicated runs were carried out for each condition for averaging the results, and the experimental error was found to be within ±4%.

2.4. Characterization. In order to determine the crystal phase composition and the crystallite size of the photocatalysts, X-ray diffraction measurement was carried out at room temperature using a DX-2000 X-ray powder diffractometer with Cu Kα radiation and a scanning speed of 3°/min. The accelerating voltage and emission current were 40 kV and 30 mA, respectively. The crystallite size was calculated by X-ray line broadening analysis using the Scherrer equation.

The microcrystalline structure and surface characteristics of the photocatalysts were also investigated by using (X-650 Japan) scanning electron microscope.

Transmission electron microscopy and high-resolution transmission electron microscopy (HR-TEM) images were performed with a JEOL-2010 transmission electron microscope, using an accelerating voltage of 200 kV.

UV-Vis diffuse reflectance spectra measurements were carried out using a Hitachi UV-365 spectrophotometer equipped with an integrating sphere attachment. The analysis range was from 250 to 650 nm, and $BaSO_4$ was used as a reflectance standard.

Photoluminescence emission spectra were recorded on a JASCO FP-6500 type fluorescence spectrophotometer over a wavelength range of 360–500 nm.

2.5. Analysis. The concentration of $Cr_2O_7^{2-}$ in the solution is determined spectrophotometrically using diphenylcarbazide reagent as a developer. The concentration of rhodamine B (RhB) in the solution is determined spectrophotometrically. The photoreduction efficiency of $Cr_2O_7^{2-}$ and the photooxidation efficiency of rhodamine B were calculated from the following expression:

$$\eta = \left[\frac{(C_0 - C_t)}{C_0}\right] \times 100\%, \quad (1)$$

where η is the photocatalytic efficiency; C_0 is the concentration of reactant before illumination; C_t is the concentration of reactant after illumination time t.

3. Results and Discussion

3.1. Characterization of Photocatalysts

3.1.1. XRD Analysis. The fixed ball milling time is 6 h. The XRD patterns of different photocatalysts are shown in Figure 1. It is clear that, when the amount of doped CuO is less than 5.0 wt.%, the diffraction peaks of CuO cannot be

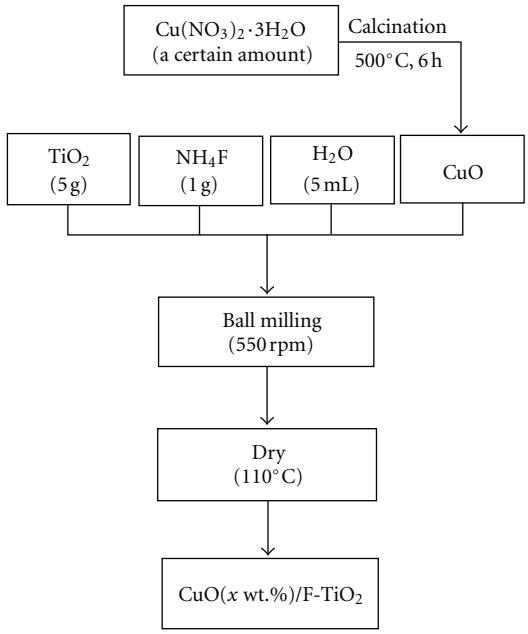

Scheme 1: The flow chart of preparation of the CuO/F-TiO_2.

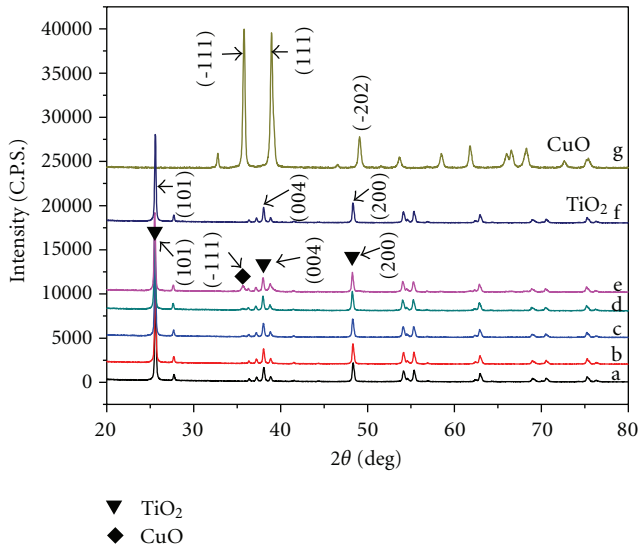

Figure 1: XRD patterns of different photocatalysts. (a) F-TiO_2, (b) CuO (0.1 wt.%)/F-TiO_2, (c) CuO (1.0 wt.%)/F-TiO_2, (d) CuO (5.0 wt.%)/F-TiO_2, (e) CuO (10.0 wt.%)/F-TiO_2, (f) TiO_2, and (g) CuO.

found in XRD patterns. This illustrates that CuO is highly dispersed in the bulk phase of the catalyst. When the amount of doped CuO is higher than 5.0 wt.%, the diffraction peaks of CuO can be found in XRD patterns. Since no new crystal phases are found, it can be concluded that a new solid is not formed in the ball milling process of TiO_2, NH_4F, and CuO, or probably because the new materials content are too low to allow detection of their reflection peaks. The similar result was reported in [30]. It is known by the calculation from the Scherrer equation that the diameter of the photocatalyst is not obviously changed. The crystallite size is about 50 nm.

3.1.2. SEM Analysis. SEM was used to investigate the morphology of the samples. Figure 2 shows SEM images of CuO (1.0 wt.%)/F-TiO_2 photocatalysts ball milled for 6 and 24 h, respectively. It can be seen that the appearance is shapeless sheet, and the average diameter of the photocatalyst is about 50–60 nm. The result is the same as that of XRD. From Figure 2, it also can be seen that, when the ball milling time is 6 h, the dispersion degree of the sample is higher than that of the sample ball milled for 24 h. Namely, when the ball milling time is longer than the optimum time, with the increase in the ball milling time, the fresh surfaces formed by

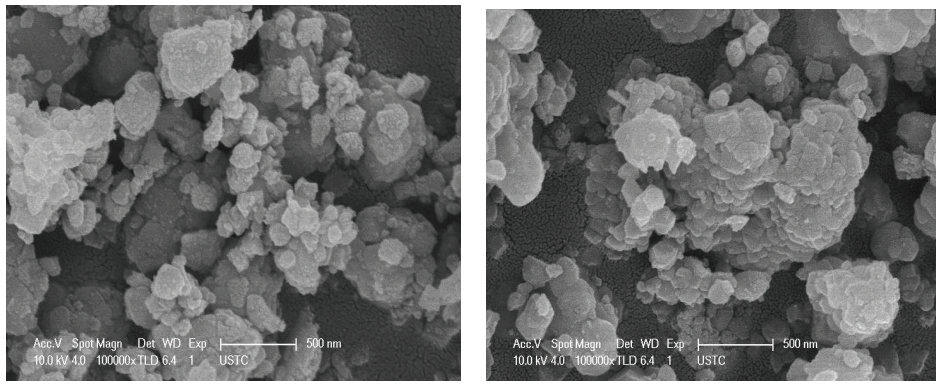

(a) (b)

Figure 2: SEM images of CuO (1.0 wt.%)/F-TiO_2 photocatalysts. (a) CuO (1.0 wt.%)/F-TiO_2, ball milling time 6 h, (b) CuO (1.0 wt.%)/F-TiO_2, ball milling time 24 h.

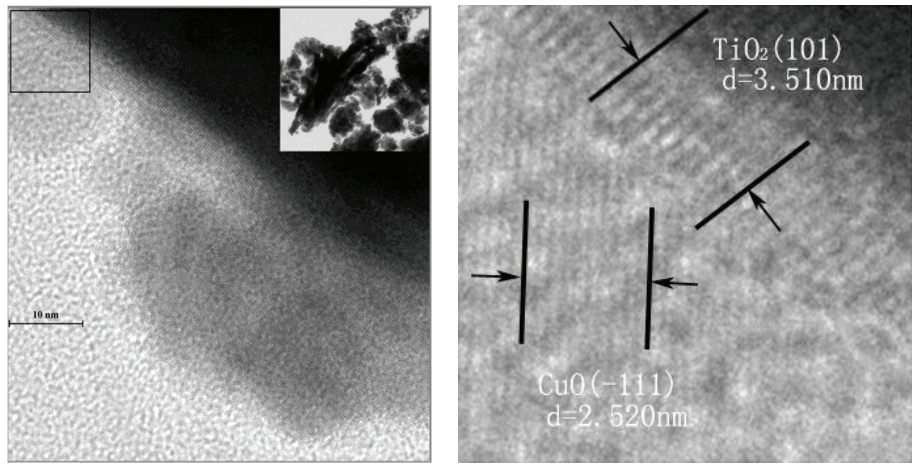

(a) (b)

Figure 3: TEM and HR-TEM images of CuO (1.0 wt.%)/F-TiO_2photocatalyst: (a) TEM image, (b) HR-TEM image.

high-energy ball milling possess high surface energy and prefer to agglomerate. The similar result was reported in [30].

3.1.3. TEM Analysis. In order to investigate the interface of the sample, the CuO (1.0 wt.%)/F-TiO_2 was chosen for TEM and high-resolution TEM characterization.

Figure 3(a) gives an overview of the typical TEM image of the CuO (1.0 wt.%)/F-TiO_2 photocatalyst. It clearly exhibits the existence of CuO nanoparticles with mean sizes of about 50–70 nm dispersing over the particle of TiO_2. Figure 3(b) shows the HR-TEM image of the sample corresponding to the rectangle region of the TEM image in Figure 3(a). The upper part depicts the (101) plane of TiO_2 with a spacing value of 3.510 nm. The lower part depicts the (−111) plane of CuO with a spacing of 2.520 nm. The good crystalline quality and the clear interface between CuO and TiO_2 are advantageous for the separation of the photogenerated charge carriers. Based on the above results, it is suggested that the heterojunction will be formed by ball milling between CuO and TiO_2.

3.1.4. UV-Vis Analysis. Figure 4 shows the UV-Vis diffuse reflectance spectra of F-TiO_2 and a series of CuO/F-TiO_2 photocatalysts. The samples were ball milled for 6 h, respectively. It is known that the bandgap of TiO_2 is about 3.2 eV and it can be excited by photons with wavelengths below 387 nm. From Figure 4, it can be seen that, compared with pure TiO_2, the absorption wavelength ranges of the F-TiO_2 and CuO/F-TiO_2 are extended greatly towards visible light. Compared with the F-TiO_2, the absorption edge of the photocatalyst CuO/F-TiO_2 extends a little to longer wavelength, revealing the good contact between CuO and F-TiO_2crystallites as a consequence of the interdispersion of the two phases produced by ball milling process. For F-TiO_2, the presence of a strong absorption band at a low wavelength in the spectra near 350 nm indicates that the Ti species are tetrahedral Ti^{4+}. This absorption band is generally

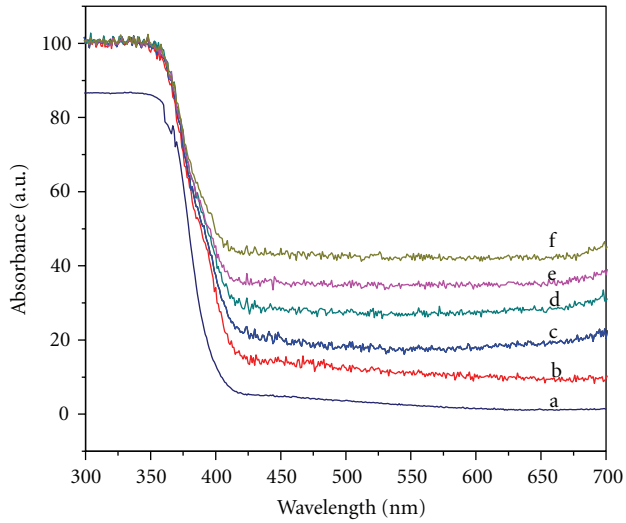

Figure 4: UV-Vis diffuse reflectance spectra of different photocatalysts. (a) TiO_2, (b) F-TiO_2, (c) CuO(0.1 wt.%)/F-TiO_2, (d) CuO(0.3 wt.%)/F-TiO_2, (e) CuO(0.5 wt.%)/F-TiO_2, (f) CuO(1 wt.%)/F-TiO_2.

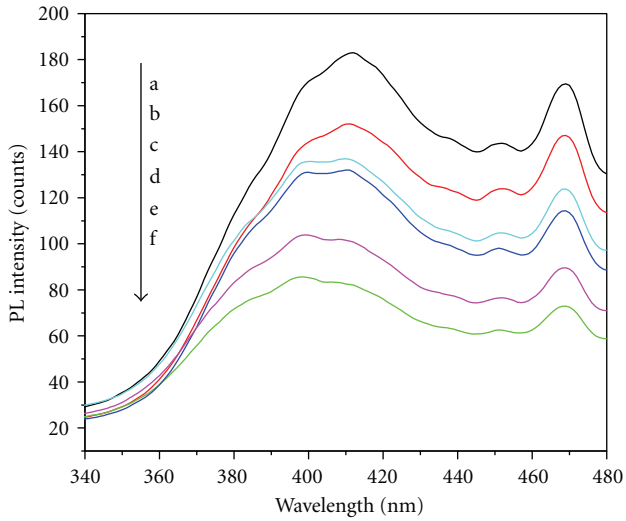

Figure 5: Photoluminescence emission spectra of photocatalysts. (a) TiO_2, (b) CuO (0.1 wt.%)/F-TiO_2, (c) CuO (0.3 wt.%)/F-TiO_2, (d) CuO (0.5 wt.%)/F-TiO_2, (e) CuO (3 wt.%)/F-TiO_2, (f) CuO (1 wt.%)/F-TiO_2.

associated with the electronic excitation of the valence band O2p electron to the conduction band Ti3d level. The photoexcited wavelength range of the CuO/F-TiO_2 photocatalyst is connected with the amount of CuO. It increases with the increase in the amount of CuO. In theory, because the absorption wavelength range is extended greatly towards visible light and the absorption intensity increases, the formation rate of electron-hole pairs on the photocatalyst surface also increases greatly, which results in the photocatalyst exhibiting higher photocatalytic activity. From Figure 7, it is clear that the photocatalytic activity of photocatalyst CuO/F-TiO_2 is strongly dependent on the amount of CuO. In the experimental condition, the results of UV-Vis diffuse reflectance spectra are consistent with the evaluation of photoreduction activity. There were similar results in previous reports [28].

3.1.5. Photoluminescence Emission Spectra. The photoluminescence emission spectra have been widely used to investigate the efficiency of charge carrier trapping, immigration, and transfer and to understand the fate of electron-hole pairs in semiconductor particles, since photoluminescence emission is resulted from the recombination of free carriers [31, 32]. In this study, using an ultraviolet light with a 260 nm wavelength as the excitation source, the fluorescence emission spectra of the different samples are shown in Figure 5. It can be seen that the samples have a stronger emission peak at around 410 nm and a weaker emission peak at around 470 nm [21, 33].

From Figure 5, it is clear that the relative intensity of the emission spectra of TiO_2 has the greatest relative intensity, which means that electrons and holes of $TiO_2$are easy to recombine. The relative intensity of the photocatalyst CuO/F-$TiO_2$is lower than that of TiO_2, showing that doping CuO is helpful to inhibit the recombination of electrons and holes and to improve the photocatalytic activity. The amount of CuO can influence the thickness of the superficial space-charge layer of TiO_2. When the amount of CuO is 1.0 wt %, the relative intensity of emission spectra is the lowest, which shows that a 1.0 wt.% doping quantity of CuO can effectively restrain the recombination of photoexcited electrons and holes. When the CuO content is too small, due to the absence of adequate traps, the recombination rate of electron-hole pairs is higher. When the doping quantity is considerably high, the absorption of light and the generation of electrons-holes are both decreased.

3.2. Evaluation of the Photocatalytic Activity

3.2.1. Effect of the Amount of NH_4F on the Photocatalytic Activity of F-TiO_2. The photocatalytic activity was investigated by photocatalytic oxidation of RhB and photocatalytic reduction of $Cr_2O_7^{2-}$. The dark absorption and blank tests are carried out simultaneously. The dark absorption test demonstrated that the adsorption on the catalysts varied depending on the samples, while the blank experiment showed that the substrate with no photocatalyst was hardly degraded after exposure to radiation for 1 h, illustrating that photoinduced self-sensitized photodegradation has little influence on the results of the experiment. All of the data obtained are corrected for absorption after stirring for 30 min in the dark. The detailed procedure was described in [34]. The fixed ball milling time is 3 h, and fixed illumination times for the photocatalytic reduction of $Cr_2O_7^{2-}$ and photocatalytic oxidation of RhB were 20 min and 10 min, respectively. Figure 6 shows the effect of the amount of NH_4F on the photocatalytic reduction of $Cr_2O_7^{2-}$ and photocatalytic oxidation of RhB.

From Figure 6, it can be seen that, without NH_4F present, namely, the pure TiO_2 powder photocatalyst, its photooxidation activity is the lowest, and the photooxidation efficiency for RhB is 15.3%. The photooxidation activity of

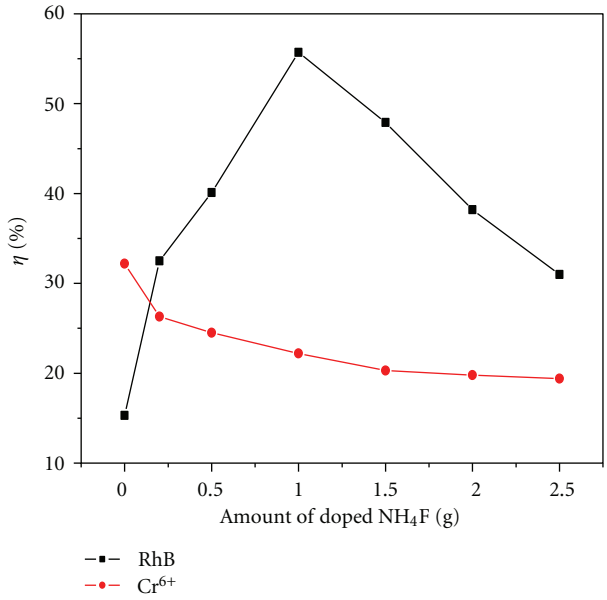

Figure 6: Effect of the amount of NH_4F on the photocatalytic reduction of $Cr_2O_7^{2-}$ and photocatalytic oxidation of RhB.

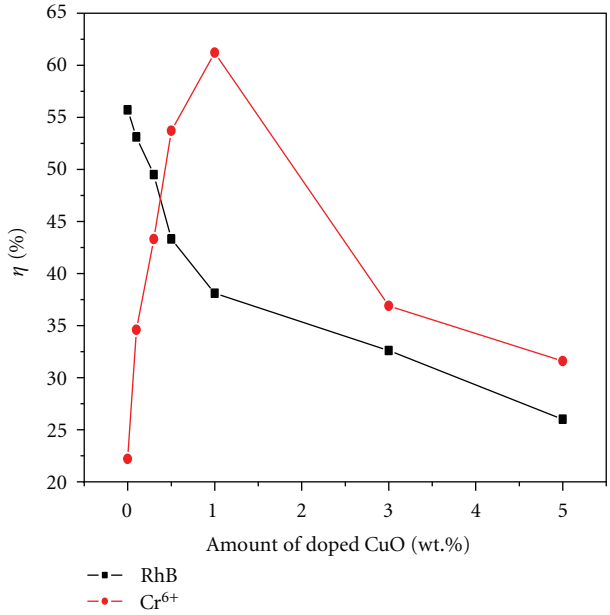

Figure 7: Effect of the amount of doped CuO on the photocatalytic reduction of $Cr_2O_7^{2-}$ and photocatalytic oxidation of RhB.

F-TiO_2 increases remarkably with the increasing amount of NH_4F up to 1.0 g. When the amount of NH_4F is 1.0 g, the photocatalytic activity of the F-TiO_2 photocatalyst is at its peak, and the photooxidation efficiency for RhB is 55.7%. When the amount of doped NH_4F is higher than optimal amount, the photooxidation activity of F-TiO_2 decreases gradually. At the same time, it is clear that the photooxidation activity of F-TiO_2 is higher than that of pure TiO_2 photocatalyst in the experimental condition. F-TiO_2 enhanced the photodegradation of RhB in aqueous solutions. It was proposed that the fluorinated surface favored the generation of free OH radicals, which was responsible for the enhanced photocatalytic oxidation activity. The result has been reported in earlier literature [27].

However, under the same condition, for the photocatalytic reduction of $Cr_2O_7^{2-}$, the photocatalytic reduction activity of F-TiO_2 decreases gradually with the increase in the amounts of doped NH_4F. For the pure TiO_2 powder photocatalyst, its photocatalytic reduction activity is at its peak, and the photocatalytic reduction efficiency is 32.2%. When the amounts of NH_4F are 0.2 and 2.0 g, the photoreduction efficiencies are 26.3 and 19.8%, respectively.

3.2.2. Effect of Amount of Doped CuO on the Photocatalytic Activity. In order to obtain the optimum concentration of CuO, the effect of the amount of CuO on the photocatalytic activity of CuO/F-TiO_2photocatalyst was studied. The experiments were carried out with different concentrations of CuO varying from 0% to 5 wt.%. Figure 7 shows the effects of the amount of doped CuO on the photocatalytic reduction of $Cr_2O_7^{2-}$ and photocatalytic oxidation of RhB. The fixed ball milling time for each sample was 3 h, and the fixed illumination times for the photocatalytic reduction of $Cr_2O_7^{2-}$ and photocatalytic oxidation of RhB were 20 min and 10 min, respectively. The amounts of TiO_2 and NH_4F were 5.0 g and 1.0 g, respectively. It can be seen that, for the photocatalytic reduction of $Cr_2O_7^{2-}$, the photoreduction activity of CuO/F-TiO_2 increases remarkably with the increase in the amount of doped CuO up to 1.0 wt.%. The optimum amount of doped CuO is 1.0 wt.%. When the amount of doped is higher than the optimal amount, the photoreduction activity of the CuO/F-TiO_2 photocatalyst decreases gradually as the amount of doped p-CuO increases. The results also show that, without CuO present, namely, the F-TiO_2 powder photocatalyst, its photoreduction activity is the lowest, and the photoreduction efficiency is 22.2%. When the amount of doped p-CuO is 1.0 wt.%, the photoreduction activity of CuO/F-TiO_2 is at its peak, and the photoreduction efficiency is 61.2%. From Figures 6 and 7, it is clear that the photoreduction activity of CuO/F-$TiO_2$is higher than that of pure TiO_2 and F-TiO_2 photocatalyst. It is proposed that, when the amount of CuO is lower than the optimum amount, the increase of the amount of CuO can increase trapping sites of the carriers, which prolongs the lifetime of the carriers, thereby improving the photocatalytic activity. The other important reason is that CuO is a p-type semiconductor. When the F-TiO_2 doped with suitable amount of p-CuO, both p-CuO and F-TiO_2 can form the p-n junction photocatalyst by ball milling. Therefore, the photoreduction activity increases [33]. But when the amount of p-CuO is higher than the optimum amount of doping, the high concentration dopant ions act as recombination centers of electrons and holes, decrease the thickness of the space-charge layer on the surface of TiO_2 particle, and reduce the photon absorption [21]. However, under the same condition, for the photocatalytic oxidation of RhB, the photooxidation activity of p-CuO/F-TiO_2 decreases rapidly with the increase

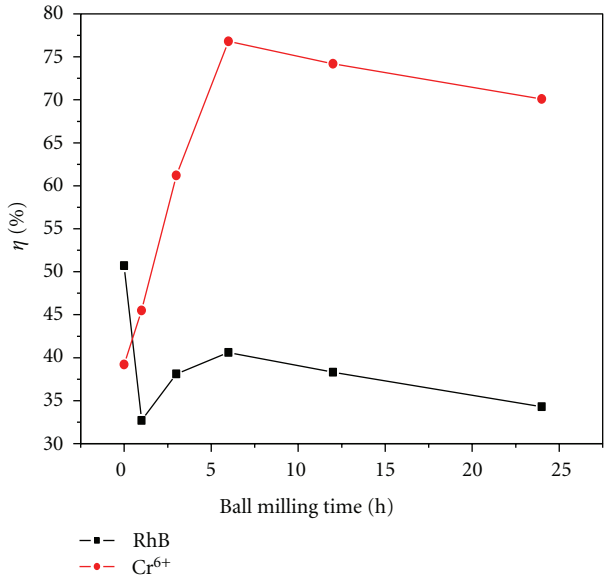

FIGURE 8: Effect of ball milling time on the photocatalytic activity.

in the amounts of doped p-CuO. For the pure F-TiO_2 photocatalyst, its photooxidation activity is at its peak, and the photooxidation efficiency of F-TiO_2 is 55.7%. When the amounts of doped p-CuO are 0.3 and 1.0 wt.%, the photooxidation efficiencies are 49.5 and 38.1%, respectively.

The photocatalyst CuO/F-TiO_2 has higher photocatalytic reduction activity than that of TiO_2 and F-TiO_2. The possible reasons are as follows.

First, it can be explained by the p-n junction principle [21, 28]. It is known that CuO is p-type semiconductor, and TiO_2 is n-type semiconductor. When p-type CuO and n-type TiO_2 integrate p-n junctions will be formed between CuO and TiO_2, and the inner electric field will be also formed at the same time in the interface. So a number of micro p-n heterojunction CuO/F-TiO_2photocatalysts will be formed after doping CuO powder into TiO_2 granule. At the equilibrium, the inner electric field formed made p-type semiconductor CuO region have the negative charge while TiO_2 region have the positive charge. The electron-hole pairs will be created under UV light illumination. With the effect of the inner electric field, the holes flow into the negative field and the electrons move to the positive field. Therefore, the photogenerated electron-hole pairs will be separated effectively by the p-n heterojunction formed in CuO/F-TiO_2.

Second, compared with F-TiO_2, the photoabsorption wavelength range of the CuO/F-TiO_2 photocatalyst red shifts and extends the wavelength range of photoexcitation and enhances the utilization of the total spectrum. The results also show that the photoluminescence emission intensity of the CuO/F-TiO_2 photocatalyst is lower than that of the pure F-TiO_2. It indicates that doping CuO is helpful to inhibit the recombination of electrons and holes and improve the photocatalytic activity. At the same time, it was reported that p-type semiconductor is a collector of photoexcited holes [35]. Therefore, there are enrichment electrons in the interface to react with $Cr_2O_7^{2-}$ adsorbed on the photocatalyst surface, so the p-n heterojunction photocatalyst CuO/F-TiO_2 has higher photocatalytic reduction activity, but lower photocatalytic oxidation activity.

3.2.3. Effect of Ball Milling Time on the Photocatalytic Activity. The effect of ball milling time on the photocatalytic activity of CuO (1.0 wt.%)/F-TiO_2 photocatalyst is shown in Figure 8. It can be seen that the ball milling time influences the photocatalytic activity strongly. Without ball milling, the photoreduction efficiency is 39.2%, and the photooxidation efficiency is 51.3%. The photoreduction efficiency of $Cr_2O_7^{2-}$ increases gradually with the increase in ball milling time up to 6 h. When the ball milling time is 1, 3, 6, 12, and 24 h, the photoreduction efficiency is 45.5, 61.2, 76.8, 74.2, and 70.1%, respectively. For the photocatalytic oxidation of RhB, the photooxidation efficiency decreases rapidly with the increase in the ball milling time. When the ball milling time is 1 h, the photooxidation efficiency is the lowest, and it is 32.7%. However, when the ball milling time is longer than 1 h, the photooxidation efficiency increases gradually with the increase in ball milling time up to 6 h. When the ball milling time is 6 h, the photooxidation efficiency of RhB is 40.6%. When the ball milling time is longer than 6 h, the photooxidation efficiency decreases gradually. The reason is that, without ball milling, F-TiO_2 and p-CuO only play their own photocatalytic role, and the p-n junction photocatalysts are not formed. However, after ball milling, TiO_2 and p-CuO can form p-n junction photocatalyst, which results in the increase of the photoreduction activity and the decrease of the photooxidation activity rapidly. Another reason is that, with the increase in the ball milling time, the specific surface area of the photocatalyst increases. Correspondingly, the number of active sites per unit weight of photocatalyst also increases [21]. But when the ball milling time is longer than the optimum time, it is proposed that, with the increase in the ball milling time, the fresh surface formed by high-energy ball milling possesses high surface energy and prefers to agglomerate [36, 37], resulting in the decrease of the photocatalytic activity. The assumption is proved by the results of SEM.

3.2.4. Hydroxyl Radical Analysis. The formation of hydroxyl radicals ($^{\bullet}OH$) on the surface of CuO (1.0 wt.%)/F-TiO_2 photocatalyst is detected by a photoluminescence (PL) technique with terephthalic acid as a probe molecule. The method is rapid, sensitive, and specific, needing only simple standard PL instrumentation. Terephthalic acid readily reacts with $^{\bullet}OH$ to produce a highly fluorescent product, 2-hydroxyterephthalic acid, whose PL peak intensity is in proportion to the amount of OH radicals produced in water. Experimental procedures were reported in earlier reports [27]. After UV irradiation for 10 min, the reaction solution was filtrated to measure the PL intensity at 425 nm excited by 315 nm light of 2-hydroxyterephthalic acid.

Figure 9 shows the changes of PL spectra of different samples from 5×10^{-4} mol/L terephthalic acid solution in 2×10^{-3} mol/L NaOH. From Figure 9, it can be seen that, when the ball milling time is 6 h, the PL peak intensity of the sample is the highest. It means that the formation rate of

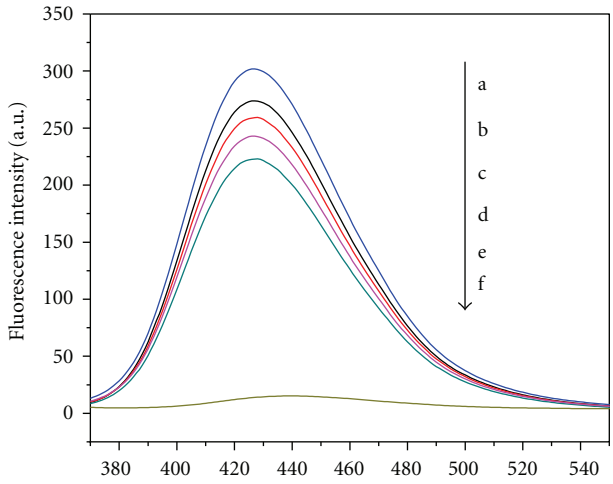

Figure 9: Effect of ball milling time on the changes of PL spectra. (a) 6 h, (b) 3 h, (c) 12 h, (d) 24 h, (e) 1 h, (f) pure terephthalic acid.

OH radicals on its surface is much larger than that of other samples. The PL peak intensities of the samples decrease are as follows: ball milling time 6 h > 3 h > 12 h > 24 h > 1 h. The result of PL peak intensity is consistent with that of the photooxidation activity.

4. Conclusions

The CuO/F-TiO_2 photocatalyst was prepared by ball milling method. The photooxidation activity of F-TiO_2 increases greatly with the increase in the amount of NH_4F up to 1.0 g. The photoreduction activity of CuO/F-TiO_2 increases remarkably with the increase in the amount of doped p-CuO up to 1.0 wt.%. The ball milling time has a significant influence on the photocatalytic activity of the photocatalyst. The optimum ball milling time is 6 h. Compared with pure TiO_2, the photoabsorption wavelength range of the F-TiO_2 and CuO/F-TiO_2 photocatalysts red shifts and improves the utilization of the total spectrum. As the formation of the p-n heterojunction and p-type CuO species acts as holes traps and collector, the photogenerated electron-hole pairs of the CuO/F-TiO_2 photocatalyst are separated by the inner electric field and the photocatalytic reduction activity is enhanced greatly.

Acknowledgments

This study was supported by the Natural Science Foundation of China (nos. 20973071, 51172086, and 21103060) and the Key Project of Science and Technology Research of Ministry of Education of China (208062).

References

[1] A. Fujishima and K. Honda, "Electrochemical photolysis of water at a semiconductor electrode," *Nature*, vol. 238, no. 5358, pp. 37–38, 1972.

[2] T. Yan, J. Long, X. Shi, D. Wang, Z. Li, and X. Wang, "Efficient photocatalytic degradation of volatile organic compounds by porous indium hydroxide nanocrystals," *Environmental Science and Technology*, vol. 44, no. 4, pp. 1380–1385, 2010.

[3] X. Xin, M. Scheiner, M. Ye, and Z. Lin, "Surface-treated TiO_2 nanoparticles for dye-sensitized solar cells with remarkably enhanced performance," *Langmuir*, vol. 27, no. 23, pp. 14594–14598, 2011.

[4] X. Xu, X. Li, P. Lin et al., "A general templated method to homogeneous and composition-tunable hybrid TiO_2 nanocomposite fibers," *Chemical Communications*, vol. 47, no. 9, pp. 2538–2540, 2011.

[5] Z. J. Zhou, J. Q. Fan, X. Wang, W. H. Zhou, Z. L. Du, and S. X. Wu, "Effect of highly ordered single-crystalline TiO_2 nanowire length on the photovoltaic performance of dye-sensitized solar cells," *ACS Applied Materials & Interfaces*, vol. 3, pp. 4349–4353, 2011.

[6] K. Lv, J. Yu, J. Fan, and M. Jaroniec, "Rugby-like anatase titania hollow nanoparticles with enhanced photocatalytic activity," *CrystEngCommunity*, vol. 13, no. 23, pp. 7044–7048, 2011.

[7] D. Yang, C. Chen, Z. Zheng et al., "Grafting silica species on anatase surface for visible light photocatalytic activity," *Energy and Environmental Science*, vol. 4, no. 6, pp. 2279–2287, 2011.

[8] Y. Wang, D. Zhao, H. Ji et al., "Sonochemical hydrogen production efficiently catalyzed by Au/TiO_2," *Journal of Physical Chemistry C*, vol. 114, no. 41, pp. 17728–17733, 2010.

[9] R. Shi, J. Lin, Y. Wang, J. Xu, and Y. Zhu, "Visible-light photocatalytic degradation of $BiTaO_4$ photocatalyst and mechanism of photocorrosion suppression," *Journal of Physical Chemistry C*, vol. 114, no. 14, pp. 6472–6477, 2010.

[10] R. J. Wang, G. H. Jiang, Y. W. Ding et al., "Photocatalytic activity of heterostructures based on TiO_2 and halloysite nanotubes," *ACS Applied Materials & Interfaces*, vol. 3, pp. 4154–4158, 2011.

[11] D. Y. Wu and M. Long, "Realizing visible-light-induced self-cleaning property of cotton through coating N-TiO_2 film and loading AgI particles," *ACS Applied Materials & Interfaces*, vol. 3, pp. 4770–4774, 2011.

[12] M. Liu, X. Qiu, M. Miyauchi, and K. Hashimoto, "Cu(II) oxide amorphous nanoclusters grafted Ti^{3+} self-doped TiO_2: an efficient visible light photocatalyst," *Chemistry of Materials*, vol. 23, no. 23, pp. 5282–5286, 2011.

[13] N. Zhang, S. Liu, X. Fu, and Y.-J. Xu, "Synthesis of M@TiO_2 (M = Au, Pd, Pt) core-shell nanocomposites with tunable photoreactivity," *Journal of Physical Chemistry C*, vol. 115, no. 18, pp. 9136–9145, 2011.

[14] T. A. Kandiel, A. A. Ismail, and D. W. Bahnemann, "Mesoporous TiO_2 nanostructures: a route to minimize Pt loading on titania photocatalysts for hydrogen production," *Physical Chemistry Chemical Physics*, vol. 13, no. 45, pp. 20155–20161, 2011.

[15] P. Sangpour, F. Hashemi, and A. Z. Moshfegh, "Photoenhanced degradation of methylene blue on cosputtered M : TiO_2 (M = Au, Ag, Cu) nanocomposite systems: a comparative study," *Journal of Physical Chemistry C*, vol. 114, no. 33, pp. 13955–13961, 2010.

[16] K. Yang, Y. Dai, and B. Huang, "Density functional study of boron-doped anatase TiO_2," *Journal of Physical Chemistry C*, vol. 114, no. 46, pp. 19830–19834, 2010.

[17] P. Xu, J. Lu, T. Xu, S. Gao, B. Huang, and Y. Dai, "I2-hydrosol-seeded growth of $(I_2)_n$-C-codoped meso/nanoporous TiO_2 for visible light-driven photocatalysis," *Journal of Physical Chemistry C*, vol. 114, no. 20, pp. 9510–9517, 2010.

[18] W. Guo, Y. Shen, L. Wu, Y. Gao, and T. Ma, "Effect of N dopant amount on the performance of dye-sensitized solar cells based on N-Doped TiO_2 electrodes," *Journal of Physical Chemistry C*, vol. 115, no. 43, pp. 21494–21499, 2011.

[19] J. Lin, J. Lin, and Y. Zhu, "Controlled synthesis of the $ZnWO_4$ nanostructure and effects on the photocatalytic performance," *Inorganic Chemistry*, vol. 46, no. 20, pp. 8372–8378, 2007.

[20] A. T. Kuvarega, R. W. M. Krause, and B. B. Mamba, "Nitrogen/palladium-codoped TiO_2 for efficient visible light photocatalytic dye degradation," *Journal of Physical Chemistry C*, vol. 115, no. 45, pp. 22110–22120, 2011.

[21] S. Chen, W. Zhao, W. Liu, and S. Zhang, "Preparation, characterization and activity evaluation of p-n junction photocatalyst p-ZnO/n-TiO_2," *Applied Surface Science*, vol. 255, no. 5, pp. 2478–2484, 2008.

[22] Z.-R. Tang, F. Li, Y. Zhang, X. Fu, and Y.-J. Xu, "Composites of titanate nanotube and carbon nanotube as photocatalyst with high mineralization ratio for gas-phase degradation of volatile aromatic pollutant," *Journal of Physical Chemistry C*, vol. 115, no. 16, pp. 7880–7886, 2011.

[23] V. Štengl, D. Popelková, and P. Vláčil, "TiO_2-graphene nanocomposite as high performace photocatalysts," *Journal of Physical Chemistry C*, vol. 115, no. 51, pp. 25209–25218, 2011.

[24] J. Zhang, J. Yu, Y. Zhang, Q. Li, and J. R. Gong, "Visible light photocatalytic H_2-production activity of CuS/ZnS porous nanosheets based on photoinduced interfacial charge transfer," *Nano Letters*, vol. 11, no. 11, pp. 4774–4779, 2011.

[25] H. Park and W. Choi, "Effects of TiO_2 surface fluorination on photocatalytic reactions and photoelectrochemical behaviors," *Journal of Physical Chemistry B*, vol. 108, no. 13, pp. 4086–4093, 2004.

[26] W. Choi, "Pure and modified TiO_2 photocatalysts and their environmental applications," *Catalysis Surveys from Asia*, vol. 10, no. 1, pp. 16–28, 2006.

[27] J. Yu, W. Wang, B. Cheng, and B. L. Su, "Enhancement of photocatalytic activity of Mesporous TiO_2 powders by hydrothermal surface fluorination treatment," *Journal of Physical Chemistry C*, vol. 113, no. 16, pp. 6743–6750, 2009.

[28] S. F. Chen, S. J. Zhang, W. Liu, and W. Zhao, "Preparation and activity evaluation of p-n junction photocatalyst NiO/TiO_2," *Journal of Hazardous Materials*, vol. 155, no. 1-2, pp. 320–326, 2008.

[29] H. Yu, J. Yu, S. Liu, and S. Mann, "Template-free hydrothermal synthesis of CuO/Cu_2O composite hollow microspheres," *Chemistry of Materials*, vol. 19, no. 17, pp. 4327–4334, 2007.

[30] S. F. Chen, L. Chen, S. Gao, and G. Y. Cao, "The preparation of nitrogen-doped photocatalyst TiO_2—XN x by ball milling," *Chemical Physics Letters*, vol. 413, no. 4-6, pp. 404–409, 2005.

[31] T. Cai, M. Yue, X. Wang, Q. Deng, Z. Peng, and W. Zhou, "Preparation, characterization, and photocatalytic performance of $NdPW_{12}O_{40}/TiO_2$ composite catalyst," *Chinese Journal of Catalysis*, vol. 28, no. 1, pp. 10–16, 2007.

[32] J. W. Tang, Z. G. Zou, and J. H. Ye, "Photophysical and photocatalytic properties of $AgInW_2O_8$," *The Journal of Physical Chemistry B*, vol. 107, pp. 14265–14269, 2003.

[33] S. Kang, K. Shin, K. Prabakar, and C. Lee, "Optical and electrical properties of ZnO doped with nitrogen," *Physica Status Solidi B*, vol. 241, no. 12, pp. 2830–2834, 2004.

[34] S. F. Chen, X. L. Yu, H. Y. Zhang, and W. Liu, "Preparation and photocatalytic activity evaluation of composite Fe-TiO_2/TiO_2 photocatalyst," *Journal of the Electrochemical Society*, vol. 157, no. 5, pp. K96–K102, 2010.

[35] A. Lohner, M. Woerner, T. Elsaesser, and W. Kaiser, "Picosecond capture of photoexcited holes by shallow acceptors in p-type GaAs," *Physical Review Letters*, vol. 68, no. 26, pp. 3920–3923, 1992.

[36] S. F. Chen, L. Chen, G. Shen, and C. Gengyu, "The preparation of coupled WO3/TiO_2 photocatalyst by ball milling," *Powder Technology*, vol. 160, no. 3, pp. 198–202, 2005.

[37] J. Wang, S. Yin, M. Komatsu, Q. Zhang, F. Saito, and T. Sato, "Preparation and characterization of nitrogen doped $SrTiO_3$ photocatalyst," *Journal of Photochemistry and Photobiology A*, vol. 165, no. 1–3, pp. 149–156, 2004.